Structural Engineering and Mechanics, *Vol. 61, No. 5 (2017) 577-592*
DOI: https://doi.org/10.12989/sem.2017.61.5.577

Prestressed concrete beams under torsion-extension of the VATM and evaluation of constitutive relationships

Luís F.A. Bernardo* and Jorge M.A. Andrade[a]

Department of Civil Engineering and Architecture, Centre of Materials and Building Technologies (C-made), University of Beira Interior, Covilhã, Portugal

(Received June 23, 2016, Revised October 17, 2016, Accepted October 21, 2016)

Abstract. A computing procedure is presented to predict the ultimate behavior of prestressed beams under torsion. This computing procedure is based on an extension of the Variable Angle Truss-Model (VATM) to cover both longitudinal and transversal prestressed beams. Several constitutive relationships are tested to model the behavior of the concrete in compression in the struts and the behavior of the reinforcement in tension (both ordinary and prestress). The theoretical predictions of the maximum torque and corresponding twist are compared with some results from reported tests and with the predictions obtained from some codes of practice. One of the tested combinations of the relationships for the materials was found to give simultaneously the best predictions for the resistance torque and the corresponding twist of prestressed beams under torsion. When compared with the predictions from some codes of practice, the theoretical model which incorporates the referred combination of the relationships provides best values for the torsional strength and leads to more optimized designs.

Keywords: PC beams; torsion; longitudinal and transversal prestress; VATM; stress-strain relationships

1. Introduction

The use of High-Strength Concrete (HSC) in Prestressed Concrete (PC) structures is becoming somehow frequent in the last years. Such structures are expected to be more flexible than Normal-Strength Concrete (NSC) structures because HSC reduces self-weight and inertia of the structural members and the increase in the Modulus of Elasticity is not sufficient to counterbalance the reduction of mass. This high flexibility could be problematic and can be solved by using prestress technique to increase the stiffness. For this purpose, the application of longitudinal prestress in members under high torsion forces is a normal situation (Navarro Gregori *et al.* 2007).

The first studies on torsion of Reinforced Concrete (RC) beams were published in the beginning of the past century. One of the developed theoretical models is the Space Truss Analogy (STA) which has an important historical value and constitutes the base of the American code (since 1995) and the European model code (since 1978). Based on the STA, several theories were developed. One of the theories widely used to compute the torsional strength is the Variable Angle Truss-Model (VATM) which gives a good physical understanding of the torsion problem in RC and PC beams. Several authors have contributed to establish the latest versions of the VATM and many studies can be found in the literature. Hsu and Mo (1985) developed a consistent model for PC beams (with longitudinal prestress) which account the influence of the softening effect. The VATM usually provides good results for high levels of loading. However, for low levels of loading, the VATM does not provide good predictions since the model assumes a fully cracked state from the beginning of the loading and it does not account for the concrete core influence. More complex theoretical models have been recently proposed by several authors (Bairan Garcia and Mari Bernat 2006a, b, Jeng and Hsu 2009, Mostofinejad and Behzad 2011). However, VATM is recognized as a simple model to predict with good accuracy the ultimate behavior of RC beams under torsion, even with compressive axial force interaction (Bernardo *et al.* 2015a, b).

Several proposals of stress (σ)-strain (ε) relationships for the materials can be found in the literature. Some of these proposals account for the softening effect (for the concrete in compression on struts) and the stiffening effect (for the reinforcement in tension). Lopes *et al.* (2015a, b) showed that the variability between these several proposals is very high, which justifies the need for evaluating these σ-ε relationships in order to establish solid conclusions. Jeng *et al.* (2011) showed the influence of the strain gradient effect in RC beams under torsion, which strongly depends on the σ-ε relationships chosen for the materials. This is also true for VATM because its theoretical results will strongly depend on the chosen σ-ε relationships for concrete and reinforcement.

This article presents a computational procedure, based on an extension of the VATM, to predict the ultimate behavior of PC beams under torsion. Both longitudinal and transversal PC beams are covered. The ultimate behavior of the beams is studied through the T (torque)-θ (twist) curves.

*Corresponding author, Assistant Professor
E-mail: lfb@ubi.pt
[a]Assistant Professor
E-mail: jandrade@ubi.pt

ISSN: 1225-4568 (Print), 1598-6217 (Online)

The theoretical results obtained from several combinations of σ-ε relationships proposed by several authors are compared with some experimental results available in the literature and also with the predictions computed by using some codes of practice.

2. Previous studies and research significance

In previous studies, some authors predicted the behavior of NSC beams with longitudinal prestress under torsion by using the VATM (Hsu and Mo 1985) or more simplified truss-models (Rahal and Collins 1996). For instance, Rahal and Collins (1996) observed that the maximum torque, both experimental and theoretical, are very similar. Hsu and Mo (1985) observed that the ultimate values of the T-θ curves, both experimental and theoretical, are also quite similar. Recently, these observations were also confirmed by Andrade *et al.* (2011), Bernardo and Lopes (2008) with other beams and by using also the VATM. However, for HSC beams Bernardo and Lopes (2011) observed that the original VATM no longer could be considered adequate since resistances are highly overestimated for HSC beams with high torsional reinforcement ratio. In fact, for HSC in compression the shape of the σ-ε curve is quite different when compared with NSC (Bernardo and Lopes 2004), leading to noticeable differences in the response of the beams under torsion even for low loading levels (Jeng *et al.* 2013). Thus, theoretical models that strongly depend of σ-ε relationships cannot be directly extrapolated from NSC to HSC, including for beams under torsion. For this reason, the original calculus procedure from VATM was reviewed by Bernardo and Lopes (2011) in order to incorporate specific σ-ε relationships for HSC. Despite having achieved better results, the authors proposed additional reduction factors for the σ-ε relationships in order to approximate even more the experimental and theoretical results for HSC beams under torsion.

In the previously referred studies the authors only tested few σ-ε relationships to characterize the behavior of the materials. In general, in previous studies different authors use different σ-ε relationships, as well as different combinations of these relationships, to model the behavior of the materials to compute theoretically the maximum torque of beams under torsion. Moreover, the majority of the older studies don't incorporate beams with HSC. In past years, new refinements have been proposed for the σ-ε relationships, mainly for concrete. For this material, new expressions to compute the reduction factors for stress and strain have been also proposed. From this perspective, the number of choices for the σ-ε relationships that can be used, which are also dictated by the possible available combinations, is very high.

For this reason, Bernardo *et al.* (2012a, b) tested several σ-ε relationships for the materials found in the literature, and different combinations of these relationships, to compute the ultimate behavior of RC beams under torsion by using VATM formulation. Among the tested models and based on several comparative analyses with experimental results, the authors found one theoretical model which provides the best predictions of the torsional strength and corresponding twist. This theoretical model is the one that incorporates the σ-ε relationship for compressed concrete in struts proposed by Belarbi and Hsu (1991) with softening coefficients proposed by Zhang and Hsu (1998) and the σ-ε relationship for ordinary reinforcement in tension proposed by Belarbi and Hsu (1994). With this theoretical model, the additional reduction factors proposed by Bernardo and Lopes (2011) were no longer need for HSC beams.

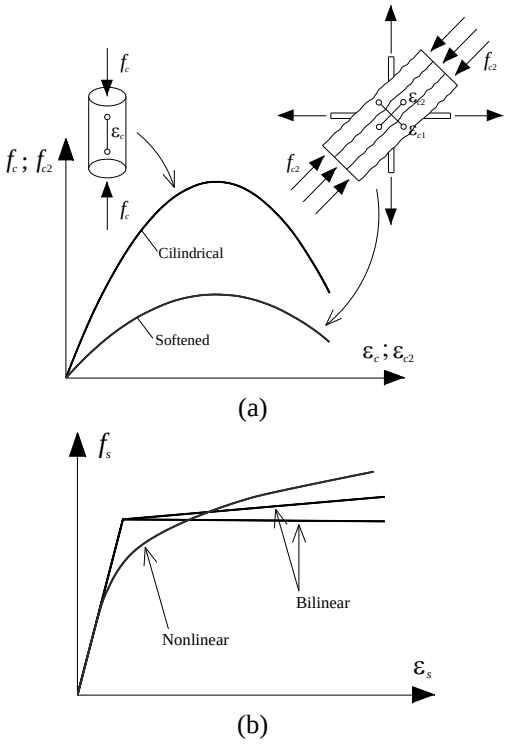

Fig. 1 σ-ε curves: (a) concrete in compression; (b) reinforcement in tension

The behavior observed for RC beams cannot be directly extrapolated for PC beams. For these beams, an additional σ-ε relationship for prestress reinforcement in tension needs to be introduced in the theoretical model. This modification should modify the response of the VATM and the σ-ε relationships for the materials, including their combinations, need to be rechecked for PC beams under torsion.

The aim of this article is to help researchers to choose the best relationships for the materials, and their combinations, to compute the ultimate behavior of PC beams under torsion. This is done by testing several possible combinations with the relationships found in literature, to compute both the ultimate torque and twist from the VATM. Furthermore, equilibrium equations of the VATM are modified in order to introduce the additional force in the prestress reinforcement.

3. Stress-strain relationships

Usually, theoretical models for the behavior of cracked RC elements under shear consider the independent behavior of concrete and reinforcement through their average σ-ε

Table 1 σ-ε relationships for concrete in compression in the struts

$f_{c2}=\beta_\sigma f_c'\left[2\left(\frac{\varepsilon_{c2}}{\beta_\varepsilon\varepsilon_o}\right)-\left(\frac{\varepsilon_{c2}}{\beta_\varepsilon\varepsilon_o}\right)^2\right]$ for $\varepsilon_{c2}\geq\beta_\varepsilon\varepsilon_o$ $f_{c2}=\beta_\sigma f_c'\left[1-\left(\frac{\varepsilon_{c2}-\beta_\varepsilon\varepsilon_o}{A\varepsilon_o-\beta_\varepsilon\varepsilon_o}\right)^2\right]$ for $\varepsilon_{c2}<\beta_\varepsilon\varepsilon_o$	Vecchio and Collins (1982), $\beta_\sigma=\beta_\varepsilon=\beta$ $A=2$ Belarbi and Hsu (1991), $A=2$ Zhu *et al.* (2001)[1]: $A=4$
Vecchio and Collins (1986), $f_{c2}=\beta_\sigma f_c'\left[2\left(\frac{\varepsilon_{c2}}{\varepsilon_o}\right)-\left(\frac{\varepsilon_{c2}}{\varepsilon_o}\right)^2\right]$	Hognestad (1952), $f_c=f_c'\left[2\left(\frac{\varepsilon_c}{\varepsilon_o}\right)-\left(\frac{\varepsilon_c}{\varepsilon_o}\right)^2\right]$
$f_{c2,base}=-f_p\frac{n\left(-\varepsilon_{c2}/\varepsilon_p\right)}{n-1+\left(-\varepsilon_{c2}/\varepsilon_p\right)^{nk}}$ $n=0.80+f_p(\text{MPa})/17$ $\begin{cases}k=1.0 & -\varepsilon_p<\varepsilon_{c2}<0\\ k=0.67+f_p(\text{MPa})/62 & \varepsilon_{c2}<-\varepsilon_p\end{cases}$	Collins and Poraz Model A (1989), i) if $-\varepsilon_{c2}\leq\beta\varepsilon_o$: $f_p=\beta f_c'$ and $\varepsilon_p=\beta\varepsilon_o$; ii) if $\beta\varepsilon_o<-\varepsilon_{c2}\leq\varepsilon_o$: $f_{c2}=f_p=\beta f_c'$; iii) if $-\varepsilon_{c2}>\varepsilon_o$: $f_{c2}=\beta f_{c2,base}$, $f_p=f_c'$ and $\varepsilon_p=\varepsilon_o$ Collins and Poraz Model B (1989), i) if $-\varepsilon_{c2}\leq\varepsilon_o$: $f_p=\beta f_c'$ and $\varepsilon_p=\varepsilon_o$; ii) if $-\varepsilon_{c2}>\varepsilon_o$: $f_{c2}=\beta f_{c2,base}$, $f_p=f_c'$ and $\varepsilon_p=\varepsilon_o$

[1] Calibrated for HSC

Table 2 Reduction factors for stress and strain

$\beta=\frac{1.0}{A-B\varepsilon_{c1}/C}$	Vecchio and Collins (1982), $\beta_\sigma=\beta_\varepsilon=\beta$ $A=0.85$ $B=0.27$ $C=\varepsilon_{c2}$ Vecchio and Collins (1986), $\beta_\sigma=\beta\leq1$ $A=0.80$ $B=0.34$ $C=\varepsilon_o$
$\beta=\frac{1.0}{1.0+K_cK_f}\leq1.0$ $K_c=A\left(\frac{\varepsilon_{c1}}{B}-C\right)^D$	Collins and Poraz-v1 (1989), $\beta_\sigma=\beta_\varepsilon=\beta$ $A=0.35$ $B=-\varepsilon_{c2}$ $C=0.28$ $D=0.8$ $K_f=0.1825\sqrt{f_c'\,(\text{MPa})}\geq1$ Collins and Poraz-v2 (1989), $\beta_\sigma=\beta$ $\beta_\varepsilon=D=1$ $A=0.27$ $B=\varepsilon_o$ $C=0.37$ $K_f=1$ Vecchio *et al.* (1994), $\beta_\sigma=\beta$ $\beta_\varepsilon=1$ $A=0.27$ $B=\varepsilon_o$ $C=0.37$ $D=1$ $K_f=2.55-0.2629\sqrt{f_c'\,(\text{MPa})}\leq1.11$
$\beta=\frac{1}{1+C_sC_d}$ $C_s=0.55$ $C_d=K_c=A\left(\varepsilon_{c1}/B-C\right)^D$	Vecchio v1 (2000), $\beta_\sigma=\beta_\varepsilon=\beta$ $A=0.35$ $B=-\varepsilon_{c2}$ $C=0.28$ $D=0.8$ Vecchio v2 (2000), $\beta_\sigma=\beta$ $\beta_\varepsilon=D=1$ $A=0.27$ $B=\varepsilon_o$ $C=0.37$
$\beta=\frac{1.0}{A+B\left(\frac{-F\varepsilon_{c1}}{C}-D\right)^E}$	Vecchio v1 (2000), $\beta_\sigma=\beta_\varepsilon=\beta\leq1$ $A=F=1$ $B=0.35$ $C=\varepsilon_{c2}$ $D=0.28$ $E=0.8$ Vecchio-v2 (2000), $\beta_\sigma=\beta\leq1$ $A=F=1$ $B=0.35$ $C=\varepsilon_{c2}$ $D=0.28$ $E=0.8$ Mikame *et al.* (1991), $\beta_\sigma=\beta_\varepsilon=\beta$ $A=0.27$ $B=0.96$ $C=\varepsilon_o$ $D=0$ $E=0.167$ $F=1$ Ueda *et al.* (1991)[1], $\beta_\sigma=\beta_\varepsilon=\beta$ $A=0.8$ $B=0.6$ $C=1$ $D=-0.2$ $E=0.39$ $F=-10^3$
Belarbi and Hsu (1991), $\beta_\sigma=0.9/\sqrt{1+400\varepsilon_{c1}}$ $\beta_\varepsilon=1/\sqrt{1+160\varepsilon_{c1}}$	$\beta_\sigma=\beta_\varepsilon=0.9/\sqrt{1+A\varepsilon_{c1}}$ Hsu (1993), $A=600$ Belarbi e Hsu (1995), $A=400$
Zhang and Hsu (1998)[1], $\beta_\sigma=\beta_\varepsilon=\frac{R(f_c')}{\sqrt{1+400\varepsilon_{c1}/\eta'}}$ $\begin{cases}\eta\leq1\Rightarrow\eta'=\eta\\ \eta>1\Rightarrow\eta'=1/\eta\end{cases}$ $R(f_c')=5.8/\sqrt{-f_c'\,(\text{MPa})}\leq0.9$	Miyahara *et al.* (1988), $\begin{cases}\beta_\sigma=1.0 & \varepsilon_{c1}\leq0.0012\\ \beta_\sigma=1.15-125\varepsilon_{c1} & 0.0012<\varepsilon_{c1}\leq0.0044\\ \beta_\sigma=0.6 & \varepsilon_{c1}>0.0044\end{cases}$

[1] Calibrated for HSC

relationships. For concrete in compression in the struts (Fig. 1(a)), the average nonlinear σ-ε relationships usually account for the softening effect (influence of the transversal tension strains) by incorporating reduction factors. For reinforcement in tension (Fig. 1(b)), some average nonlinear σ-ε relationships account for the stiffening effect (interaction between reinforcement and concrete in tension between cracks). Other simplified σ-ε relationships (bilinear) for reinforcement don't incorporate this interaction and are simply defined from uniaxial tensile tests (Fig. 1(b)).

Table 1 presents the equations for several σ-ε relationships for concrete in compression in the struts found in the literature. They will be checked in this study. Table 2 presents the equations for the reduction factors for stress (β_σ) and strain (β_ε) also proposed by several authors. The

Table 3 Tested σ-ε relationships for concrete in compression in the struts

Model	σ-ε relationship	Reduction factores β_σ and β_ε
*c*01	Hognestad (1952)	-
*c*02	Vecchio and Collins (1982)	Vecchio and Collins (1982)
*c*03	Vecchio and Collins (1986)	Vecchio and Collins (1986)
*c*04	Collins and Poraz -Model A (1989)	Collins and Poraz (1989)
*c*05	Collins and Poraz -Mod. B (1989)	Collins and Poraz (1989)
*c*06	Collins and Poraz -Model A (1989)	Vecchio *et al.* (1994)
*c*07	Collins and Poraz -Model A (1989)	Vecchio -v1 (2000)
*c*08	Collins and Poraz -Mod. B (1989)	Vecchio -v2 (2000)
*c*09	Vecchio and Collins (1982)	Vecchio -v1 (2000)
*c*10	Vecchio and Collins (1986)	Vecchio -v2 (2000)
*c*11	Belarbi and Hsu (1991)	Belarbi and Hsu (1991)
*c*12	Belarbi and Hsu (1991)	Belarbi and Hsu (1995)
*c*13	Belarbi and Hsu (1991)	Hsu (1993)
*c*14	Belarbi and Hsu (1991)	Zhang and Hsu (1998)
*c*15	Zhu *et al.* (2001)	Zhang and Hsu (1998)
*c*16	Vecchio and Collins (1982)	Mikame *et al.* (1991)
*c*17	Vecchio and Collins (1986)	Mikame *et al.* (1991)
*c*18	Vecchio and Collins (1982)	Ueda *et al.* (1991)
*c*19	Vecchio and Collins (1986)	Ueda *et al.* (1991)
*c*20	Vecchio and Collins (1982)	Miyahara *et al.* (1988)
*c*21	Vecchio and Collins (1986)	Miyahara *et al.* (1988)

meanings of some of the principal parameters are: ε_o is the strain corresponding to the peak stress (f_c'), ε_{c1} is the principal tension strain ($\varepsilon_{c1}=\varepsilon_l+\varepsilon_t+\varepsilon_d$, Hsu, 1984), ε_l, ε_t and ε_d will be defined later, $\varepsilon_c = \varepsilon_{c2}$ is the principal compression strain in the principal direction of the compression stress ($f_c = f_{c2}$). Table 3 presents all the used combinations (c_i) between σ-ε relationships and reduction factors, accounting for the original correspondence between each other.

Table 4 presents the equations for the σ-ε relationships for ordinary (*orj*) and prestress (*prj*) reinforcement in tension to be checked in this study. The meaning of some of the main parameters are: f_s and f_p are the tensile stress, f_{sy} is the yielding stress, $f_{p0.1\%}$ is the stress corresponding to the conventional strain $\varepsilon_{p0.1\%}=0.1\%$, f_{st} and f_{pt} are the tensile strength, ε_s and ε_p are the tension strain, ε_{sy} is the yielding strain at the end of the elastic behavior, ε_{su} and ε_{pu} are the ultimate strain, E_s and E_p are the Young's Modulus.

Each model *c*01 to *c*21 (Table 3) will be used separately with models *or*1+*pr*1, *or*2+*pr*2 and *or*3+*pr*3 (Table 4). For models *c*14 and *c*15 the reduction factors $\beta_\sigma=\beta_\varepsilon$ depend on the parameter η, which represents the ratio between the resisting forces in the longitudinal and transversal reinforcement. For prestressed beams, parameter η should also account for the resistance force in the prestressed reinforcement. For beams with longitudinal and transversal prestress, parameter η is calculated as follows:

$$\eta = \frac{\rho_l f_{sly} + \rho_{pl} f_{pl0.1\%}}{\rho_t f_{sty} + \rho_{pt} f_{pt0.1\%}} = \frac{A_l f_{sly} + A_{pl} f_{pl0.1\%}}{u \frac{A_t}{s} f_{sty} + u_p \frac{A_{pt}}{s_p} f_{pt0.1\%}} \quad (1)$$

Where:

ρ_l, ρ_t = longitudinal and transversal ordinary reinforcement ratio;

ρ_{pl}, ρ_{pt} = longitudinal and transversal prestress reinforcement ratio;

A_l, A_{pl} = total area of the longitudinal ordinary and prestress reinforcement;

A_t, A_{pt} = area of one leg of the transversal ordinary and prestress reinforcement;

s_t, s_p = transversal reinforcement spacing (ordinary and prestress);

u_t, u_p = perimeter of the transversal ordinary and prestress reinforcement ($u=2x_1+2y_1$,with x_1 and y_1 the minor and major dimension of the hoop);

f_{sly}, f_{sty} = yielding stress of the longitudinal and transversal ordinary reinforcement;

$f_{pl0.1\%}$, $f_{pt0.1\%}$ = conventional stress of the longitudinal and transversal prestress reinforcement.

From the above it can be stated that, along the past years, authors have proposed different σ-ε relationships to model the behavior of the materials. Several refinements have been proposed for the σ-ε relationships, mainly for the concrete. For this material, different expressions to compute the reduction factors for stress and strain have been also proposed. From this perspective, the number of choices for the relationships that can be used, which are also dictated by the possible available combinations between them (for different reduction factors and different materials), is high. Moreover, some of these proposals (the older ones) don't cover HSC and then are not valid for HSC beams. For this reasons, to compute the ultimate behavior of PC beams under torsion, researchers can show some difficulty to choose the best σ-ε relationships and their combinations, to characterize the behavior of the materials.

4. Theoretical model based on VATM

After the decompression of concrete, a PC beam under torsion behaves like a common RC beam. Thus, prestress only influence equilibrium equations in the prestress direction (longitudinal and/or transversal). The unique modification to the equilibrium equations of VATM, as stated by Hsu and Mo (1985), is to add the force in the prestress reinforcement. This was made by the referred authors for beams with longitudinal prestress. In this study, the equations of VATM will be rewritten for the general case of beams with longitudinal and/or transversal prestress.

To compute the theoretical T-θ curve of PC beams from the VATM (Fig. 2) the three following equilibrium equations are required to compute the torque, T, the effective thickness of the walls (struts), t_d, for the equivalent tubular section and the angle of the concrete struts, α, from

Table 4 σ-ε relationships for reinforcement in tension

Ordinary reinforcement	Prestress reinforcement
Model *or*1: EC2 (2010) - Bilinear $f_s = E_s\varepsilon_s$ for $\varepsilon_s \le \varepsilon_{sy} = f_{sy}/E_s$ $f_s = \frac{f_{sy}(k-1)}{\varepsilon_{su}-\varepsilon_{sy}}\varepsilon_s$; $k = f_{st}/f_{sy}$ for $\varepsilon_{sy} < \varepsilon_s \le \varepsilon_{su}$	Model *pr*1: EC2 (2010) - Bilinear $f_p = E_p\varepsilon_p$ for $\varepsilon_p \le \varepsilon_{p0.1\%} = f_{p0.1\%}/E_p$ $f_p = \frac{f_{pt}-f_{p0.1\%}}{\varepsilon_{pu}-\varepsilon_{p0.1\%}}\varepsilon_p$ for $\varepsilon_{p0.1\%} < \varepsilon_p \le \varepsilon_{pu}$
Model *or*2: EC2 (2010) - Bilinear $f_s = E_s\varepsilon_s$ para $\varepsilon_s \le \varepsilon_{sy} = f_{sy}/E_s$ $f_s = f_{sy}$ para $\varepsilon_s > \varepsilon_{sy}$	Model *pr*2: EC2 (2010) - Bilinear $f_p = E_p\varepsilon_p$ for $\varepsilon_p \le \varepsilon_{p0.1\%} = f_{p0.1\%}/E_p$ $f_s = f_{p0.1\%}$ para $\varepsilon_p > \varepsilon_{p0.1\%}$
Model *or*3: Belarbi and Hsu (1994) - Nonlinear $f_s = \frac{0.975E_s\varepsilon_s}{\left[1+\left(1.1E_s\varepsilon_s/f_{sy}\right)^m\right]^{1/m}} + 0.025E_s\varepsilon_s$ $B = \frac{1}{\rho}\left(\frac{f_{cr}}{f_{sy}}\right)^{1.5}$ $m = 1/(9B-0.2) \le 25$ $f_{cr} = 3.75\sqrt{f_c'(psi)}$	Model *pr*2: Hsu and Mo (1985) - Nonlinear $f_p = E_p\varepsilon_p$ for $\varepsilon_p \le \varepsilon_{p0.1\%} = f_{p0.1\%}/E_p$ $f_p = \frac{E_p\varepsilon_p}{\left[1+\left(E_p\varepsilon_p/f_{pt}\right)^{4.38}\right]^{1/4.38}}$ for $\varepsilon_{p0.1\%} < \varepsilon_p \le \varepsilon_{pu}$ (Ramberg-Osgood curve)

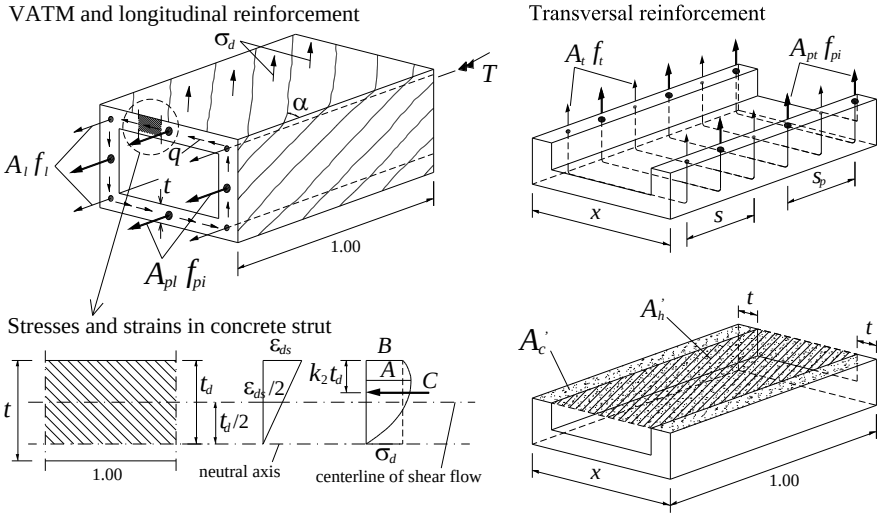

Fig. 2 VATM and strain/stress state in the concrete struts

the longitudinal axis of the beam (Hsu and Mo 1985)

$$T = 2A_o t_d \sigma_d \; sin\,\alpha \cos\alpha \tag{2}$$

$$cos^2\alpha = \frac{A_l\sigma_l + A_{pl}\sigma_{pl}}{p_o\sigma_d t_d} \quad \text{, or} \tag{3}$$

$$sin^2\alpha = \frac{A_t f_t}{s\sigma_d t_d} \tag{4}$$

$$t_d = \frac{A_l\sigma_l + A_{pl}\sigma_{pl}}{p_o\sigma_d} + \frac{A_t\sigma_t}{s\sigma_d} \tag{5}$$

Where:

A_o = area limited by the center line of the flow of shear stresses which coincides with the center line of the walls thickness, t_d;

p_o = perimeter of area A_o;

σ_d = stress in the diagonal concrete strut;

σ_l = stress in the longitudinal reinforcement;

σ_t = stress in the transversal reinforcement;

σ_{pl} = stress in the longitudinal prestress reinforcement.

It should be noted that for longitudinal prestress, the longitudinal force should include both the ordinary and prestress longitudinal reinforcement ($A_l\sigma_l$+$A_{pl}\sigma_{pl}$).

No studies were found in the literature related with the study of beams with transversal prestress by using VATM. For such beams, Eq. (4) must be rewritten in order to replace the transversal force (per unit length) in the ordinary reinforcement ($A_l\sigma_l/s$) by the total transversal force (also per unit length) including both the ordinary and prestress reinforcement ($A_l\sigma_l/s$ +$A_{pl}\sigma_{pl}/s_p$)

$$sin^2\alpha = \frac{A_t\sigma_t}{s\sigma_d t_d} + \frac{A_{pt}\sigma_{pt}}{s_p\sigma_d t_d} \tag{6}$$

Where σ_{pt} is the stress in the transversal prestress reinforcement.

For beams with longitudinal and transversal prestress, Eq. (3) and Eq. (6) should be used in order to incorporate both longitudinal and transversal force in the prestress reinforcement. In order to use one simple equation to calculate α for such beams and to generalize this equation for RC beams or PC beams with longitudinal and/or transversal prestress, an alternative and general equation is

derived here by dividing Eq. (6) by Eq. (3). This new equation substitutes Eqs. (3)-(4) and Eq. (6).

$$tg^2\alpha = \frac{sin^2\alpha}{cos^2\alpha} = \frac{\frac{A_t\sigma_t}{s} + \frac{A_{pt}\sigma_{pt}}{s_p}}{\frac{A_l\sigma_l}{p_o} + \frac{A_{pl}\sigma_{pl}}{p_o}} \quad (7)$$

Similarly, since longitudinal equilibrium equation is also used to compute the effective depth of the concrete struts (t_d), Eq. (5) should also incorporate both the total longitudinal and transversal force (general case)

$$t_d = \frac{A_l\sigma_l}{p_o\sigma_d} + \frac{A_t\sigma_t}{s\sigma_d} + \frac{A_{pl}\sigma_{pl}}{p_o\sigma_d} + \frac{A_{pt}\sigma_{pt}}{s_p\sigma_d} \quad (8)$$

For RC beams the three following compatibility equations are also need to compute the strain of the longitudinal reinforcement, ε_l, the strain of the transversal reinforcement, ε_t, and the twist, θ (Hsu and Mo 1985)

$$\varepsilon_l = \left(\frac{A_o^2\sigma_d}{p_o T\ cotg\ \alpha} - \frac{1}{2} \right) \varepsilon_{ds} \quad (9)$$

$$\varepsilon_t = \left(\frac{A_o^2\sigma_d}{p_o T\ tg\ \alpha} - \frac{1}{2} \right) \varepsilon_{ds} \quad (10)$$

$$\theta = \frac{\varepsilon_{ds}}{2t_d\ sin\alpha\ cos\alpha} \quad (11)$$

The strain at the surface of the diagonal concrete strut, ε_{ds}, and at the center line of the flow of shear stresses, ε_d, can be computed from (Fig. 2) (Hsu and Mo 1985)

$$\varepsilon_{ds} = \frac{2p_o t_d}{A_o}(\varepsilon_t + \varepsilon_d)\ tg\ \alpha\ sin\ \alpha\ cos\alpha \quad (12)$$

$$\varepsilon_d = \varepsilon_{ds}/2 \quad (13)$$

For beams with longitudinal prestress, the procedure to compute the strain and stress in the longitudinal prestress reinforcement, ε_{pl} and σ_{pl}, is the following one (Hsu and Mo 1985)

$$\varepsilon_{pl} = \varepsilon_{dec,l} + \varepsilon_l \quad (14)$$

$$\varepsilon_{dec,l} = \varepsilon_{pi,l} + \varepsilon_{li} \quad (15)$$

$$\varepsilon_{pi,l} = \frac{f_{pi,l}}{E_{pl}} \quad (16)$$

$$\varepsilon_{li} = \frac{A_{pl} f_{pi,l}}{A_l(E_s - E_c) + (A_c - A_h - A_{pl})E_c} \quad (17)$$

Where

$\varepsilon_{dec,l}$ = strain in the longitudinal prestress reinforcement at decompression;

ε_{li} = initial strain in the longitudinal ordinary reinforcement due to prestress;

$\varepsilon_{pi,l}$ = initial strain in the longitudinal prestress reinforcement due to prestress;

$f_{pi,l}$ = initial stress in the longitudinal prestress reinforcement;

E_{pl} = Young's modulus of the longitudinal prestress reinforcement;

E_c = Young's modulus of the concrete;

A_c = area limited by the external perimeter of the cross section;

A_h = Area of the hollow part of the cross section (for plain cross sections: A_h=0).

In Eq. (14) the strain in the longitudinal ordinary reinforcement, ε_l, is computed from Eq. (9).

For beams with transversal prestress, the earlier procedure should be rewritten to compute the strain in the transversal prestress reinforcement, ε_{pt}, to compute subsequently the stress σ_{pt}

$$\varepsilon_{pt} = \varepsilon_{dec,t} + \varepsilon_t \quad (18)$$

$$\varepsilon_{dec,t} = \varepsilon_{pi,t} + \varepsilon_{ti} \quad (19)$$

$$\varepsilon_{pi,t} = \frac{f_{pi,t}}{E_{pt}} \quad (20)$$

$$\varepsilon_{ti} = \frac{2\frac{A_{pt}}{s_p} f_{pi,t}}{2\frac{A_t}{s}(E_s - E_c) + \left(A_c' - A_h' - 2\frac{A_{pt}}{s_p} \right) E_c} \quad (21)$$

Where:

$\varepsilon_{dec,t}$ = strain in the transversal prestress reinforcement at decompression;

ε_{ti} = initial strain in the transversal ordinary reinforcement due to prestress;

$\varepsilon_{pi,t}$ = initial strain in the transversal prestress reinforcement due to prestress;

$f_{pi,t}$ = initial stress in the transversal prestress reinforcement;

E_{pt} = Young's modulus of the transversal prestress reinforcement.

In Eq. (18) the strain in the transversal ordinary reinforcement, ε_t, is computed from Eq. (10).

Eq. (21) can be derived assuming a beam (with unitary length) with transversal prestress in the vertical walls (Fig. 2). The total area, per unit length, of transversal ordinary and prestress reinforcement (2 vertical units per transversal section) is $2A_t/s$ and $2A_{pt}/s_p$, respectively. The horizontal area of homogenized concrete is

$$A_{c,\text{hom}} = 2\frac{A_t}{s}\frac{E_s}{E_c} + A_c' - A_h' - 2\frac{A_{pt}}{s_p} - 2\frac{A_t}{s} \quad (22)$$

Where $A_c' = x \times 1$ and $A_h' = (x - 2t) \times 1$ (see Fig. 2).

The initial transversal prestress force is calculated from

$$F_{pi,t} = 2\frac{A_{pt}}{s_p} f_{pi,t} \quad (23)$$

The initial strain in the transversal ordinary reinforcement due to transversal prestress is

$$\varepsilon_{ti} = \frac{F_{pi,t}}{E_c A_{c,\text{hom}}} \quad (24)$$

Introducing Eq. (23) and Eq. (22) into Eq. (24) leads to Eq. (21).

For transversal prestress in the horizontal walls, Eq. (21) remains valid if the average stress in the concrete due to prestress is the same as for the vertical walls.

For beams with longitudinal and transversal prestress, Eq. (14) and Eq. (18) should be used together.

The stress of the inclined concrete struts, σ_d, is defined as the medium stress of a non-uniform diagram (Fig. 2)

$$\sigma_d = k_1 \beta_\sigma f_c' \quad (25)$$

Where k_1 is the ratio between the medium stress (*B*, see Fig. 2) and the maximum stress (*A*, see Fig. 2). Parameter k_1 will be calculated by numerical integration from the σ-ε relationships for the concrete struts (Table 1).

Based on a strain state analysis, it can be demonstrated that the principal strain in tension (ε_{c1}) in the concrete strut (tension strain perpendicular to the concrete strut), to be introduced in equations for β_σ and β_ε on Table 2, can be approximately calculated from (Hsu 1984)

$$\varepsilon_{c1} = \varepsilon_l + \varepsilon_t + \varepsilon_d \quad (26)$$

The previous equations and the equations incorporated in Tables 1-3 lead to the iterative calculus procedure presented in Fig. 3 (for the general case with $\beta_\sigma \neq \beta_\varepsilon$) in order to calculate the theoretical T-θ curve of a beam with longitudinal and transversal prestress (general case). In this calculus procedure the variable t_d, α, β_σ and β_ε (if $\beta_\sigma \neq \beta_\varepsilon$) are unknown and interdependent.

Parameter ε_o was calculated from EC2 (2010). The theoretical failure of the sections was defined from the maximum strains of the materials (concrete and steel). Either the strain of the concrete struts, ε_{ds} (Fig. 2), reaches its maximum value (ε_{cu}) or the steel strain, ε_s, reaches the usual maximum value of $\varepsilon_s = 10^0/_{00}$. Parameter ε_{cu} was calculated from EC2 (2010).

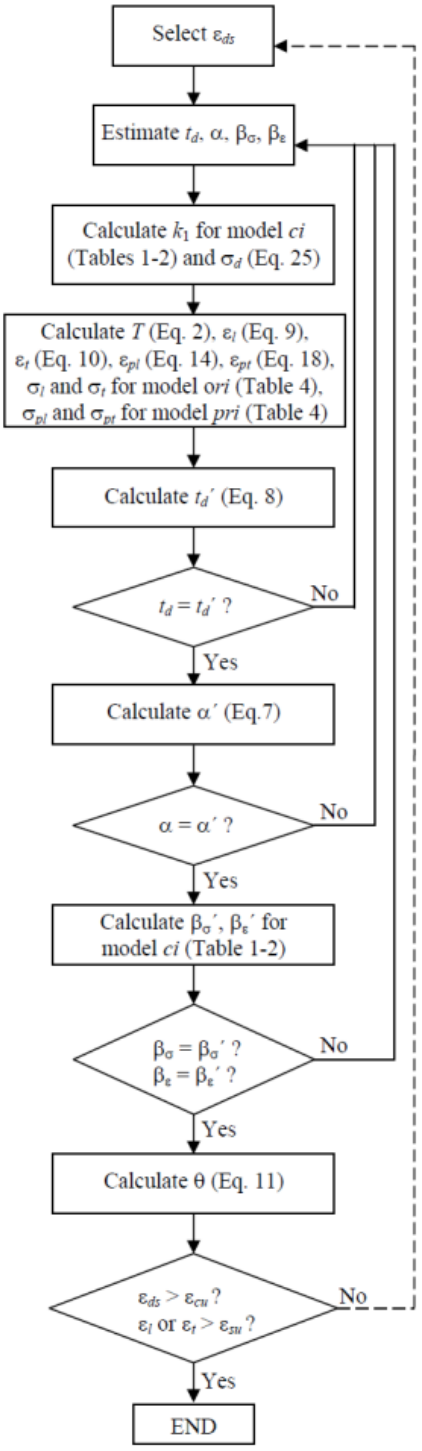

Fig. 3 Flowchart for the calculation of T-θ curve

5. Test beams

In this study, a comparative analysis focused on the ultimate behavior is carried out with the help of some experimental results of PC beams under torsion, which are available in the literature. Only beams with uniform longitudinal prestress were analyzed since no experimental tests of beams with transversal prestress were found in the literature.

The same beams used by Bernardo and Lopes (2011) and Jeng *et al.* (2010) in their comparative analysis are used in this section: Beams P2 and P3 from Mitchell and Collins (1974), Beam P8 from Hsu and Mo (1985), Beams D1 and D2 from Bernardo and Lopes (2011), Beams PA1R, PA2, PA3, PA4, PB1, PB2, PB3, PB4, PC1, PC2, PC3 and PC4 from McMullen and El-Degwy (1985). Only 3 beams were hollow (P2, D1 and D2).

It should be noted that, as justified by Bernardo and Lopes (2008, 2011), not all the experimental results available in the literature can be used for comparative analysis with theoretical results from VATM due to various reasons. For instance, some older studies have not sufficient

Table 5 Properties of reference beams

Beam	Section type	x cm	y cm	t cm	x_1 cm	y_1 cm	A_{sl} cm^2	A_{st}/s cm^2/m	A_p cm^2	ρ_l %	ρ_t %	f_{cm} MPa	f_{lym} MPa	f_{tym} MPa	$f_{p0,1\%}$ MPa	f_{pi} MPa	f_{cp} MPa	E_p GPa
P3	Plain	35.6	43.1	-	29.2	36.8	4.3	7.4	4.3	0.3	0.6	34.0	328	328	1476	1145	0.86	195
P8	Plain	25.4	38.1	-	21.6	34.3	5.2	22.6	5.2	0.5	2.6	31.0	334	336	959	690	6.83	205
PA1R	Plain	25.4	25.4	-	22.2	22.2	2.9	4.9	0.9	0.4	0.7	43.6	435	310	1638	1207	1.74	189
PA2	Plain	25.4	25.4	-	21.6	21.6	5.1	9.1	1.5	0.8	1.2	45.6	483	310	1663	1207	2.81	195
PA3	Plain	25.4	25.4	-	21.9	21.9	7.9	8.9	2.2	1.2	1.2	41.8	389	435	1744	1303	4.42	199
PA4	Plain	25.4	25.4	-	21.9	21.9	11.4	13.0	3.0	1.8	1.8	42.2	419	435	1709	1303	6.00	192
PB1	Plain	17.8	35.6	-	14.6	32.4	2.9	4.9	0.9	0.5	0.7	45.8	435	310	1638	1207	1.77	189
PB2	Plain	17.8	35.6	-	14.0	31.8	5.1	9.1	1.5	0.8	1.3	45.8	483	310	1663	1207	2.86	195
PB3	Plain	17.8	35.6	-	14.3	32.1	7.9	8.4	2.2	1.3	1.2	43.5	389	435	1744	1303	4.50	199
PB4	Plain	17.8	35.6	-	14.3	32.1	11.4	11.9	3.0	1.8	1.7	45.5	419	435	1709	1303	6.11	192
PC1	Plain	14.6	43.8	-	11.4	40.6	2.9	4.2	0.9	0.5	0.7	42.2	435	310	1638	1207	1.76	189
PC2	Plain	14.6	43.8	-	10.8	40.0	5.1	7.9	1.5	0.8	1.3	45.1	483	310	1663	1207	2.83	195
PC3	Plain	14.6	43.8	-	11.1	40.3	7.9	7.5	2.2	1.2	1.2	41.3	389	435	1744	1303	4.46	199
PC4	Plain	14.6	43.8	-	11.1	40.3	11.4	11.0	3.0	1.8	1.8	42.1	419	435	1709	1303	6.05	192
P2	Hollow	35.6	43.1	8.9	31.2	38.9	5.7	7.4	5.7	0.4	0.7	32.9	407	407	1476	1145	4.89	195
D1	Hollow	60.0	60.0	11.4	54.3	54.2	23.8	11.2	4.2	0.7	0.7	80.8	724	715	1670	640	1.79	195
D2	Hollow	60.0	60.0	11.5	55.5	55.5	23.8	11.2	5.6	0.7	0.7	58.8	724	715	1670	1100	3.08	195

data or do not meet basic design recommendations incorporated in current codes of practice. In this earlier situation, such beams show atypical behaviors under torsion. In other experimental studies, including recent studies, the authors present an average twist for all the beam length, and not the twist in the failure region (which is localized along a small length of the beam). This aspect is particularly important in slender beams. This invalidate direct comparisons between experimental twists and theoretical twists. In fact, these last are based on a theoretical section analysis (of the critical section), and not an overall analysis of the test beams. For this last reason, test beams from Wafa *et al.* (1995) (Beams H3AR, H2A, H1AR, H3B, H2B, H1B, M3A, M2A, M1A, M3B, M2B and M1B) were not be considered for some of the comparative analysis performed in this study. In many previous studies, authors only studied the resistance torque, for which this last issue is not limiting. So they could include more experimental beams in their comparative analysis. In this study, since both resistance torque and corresponding twist is studied, a much more limited number of experimental results can be used.

Table 5 summarizes some of the geometrical and mechanical properties of the test PC beams (longitudinal prestress) necessary to compute the T-θ curve, including the external width (x) and height (y) of the cross-section, the thickness of the walls of hollow sections (t), the distances between centerlines of legs of the closed stirrups (x_1 and y_1), the total area of longitudinal reinforcement (A_{sl}), the distributed area of the transversal reinforcement (A_{st}/s, where s is the spacing of transversal reinforcement), the ordinary longitudinal reinforcement ratio ($\rho_l=A_{sl}/A_c$), with $A_c=xy$) and the ordinary transversal reinforcement ratio ($\rho_t=A_{st}u/(A_cs)$, with $u=2(x_1+y_1)$, the average concrete compressive strength (f_{cm}), the average yielding stress of longitudinal and transversal ordinary reinforcement (f_{lym} and f_{tym}).

Table 5 also incorporate information about longitudinal prestress, namely: the total area of longitudinal prestress reinforcement (A_p), the proportional conventional limit stress to 0.1% ($f_{p0.1\%}$), the initial stress in the prestress reinforcement (f_{pi}), the average stress in the concrete due to prestress (f_{cp}) and the Young's modulus for the prestress reinforcement (E_p). Despite plain and hollow beams generally behaves differently (Valipour and Foster 2010, Alnuaimi *et al.* 2008), for torsion and for the resistance torque there is no noticeable diferences since the concrete core is not efective (Hsu 1984). For this reason, plain and hollow beams are grouped in the same table.

6. Comparative analysis with experimental results

Based on the computing procedure presented in Fig. 3, a computer tool was developed with the computer program language Delphi to compute the T-θ curve for PC beams under torsion (Andrade *et al.* 2011). The ultimate part of the computed theoretical curve is compared with the experimental ones from the test beams. Each one of the σ-ε relationships for concrete strut (models *c*01 to *c*21, see Table 3) and for tension steel (models *or1* to *or*3 and *pr*1 to *pr*3, see Table 4) was used. Each model *ci* (*i*=1 to 21) was combined with each model *orj*+*prj* (*j*=1 to 3) to calculate the theoretical T-θ curves. Then, 21×3=66 simulations were performed for each beam.

From the theoretical curves, the theoretical values for the maximum (resistance) torque ($T_{n,th}$) and the corresponding theoretical twist ($\theta_{n,th}$) were highlighted. This would help comparative analyses to be done on the behavior of the corresponding experimental values ($T_{n,exp}$ and $\theta_{n,exp}$). In order to facilitate the comparative analysis,

the ratios of experimental to theoretical values of the referred parameters were calculated ($T_{n,exp}/T_{n,th}$ and $\theta_{n,exp}/\theta_{n,th}$).

Table 6 summarizes the results and the comparative analyses for the parameters previously mentioned. For each parameter, three statistical parameters were quantified: the average value ($\bar{x}$), the sample standard deviation (s) and the coefficient of variation (cv).

A global analysis of Table 6 shows that the variability between the results for each tested model is higher for the twists when compared with the maximum torques. Table 6 shows that the range of values for the average $T_{n,exp}/T_{n,th}$ ratio ($\bar{x}$) is 0.75 to 1.10. The distance between extremes values is somewhat high. Model c1 shows the lower values for $\bar{x}$. This model does not incorporate reduction factors to account for the softening effect. As a consequence, the resistances are overestimated (softening effect reduces the compressive strength of concrete struts). From Table 6, it can be stated that the concrete models *c*03, *c*05, *c*06, *c*11, *c*12, *c*13, *c*14, *c*15, *c*18, *c*19, *c*20 and *c*21 are those for which $\bar{x}$ values are the closest to 1.00 (between 0.90 and 1.10). Among the referred models, models *c*11, *c*12, *c*13, *c*18 and *c*19 show $\bar{x}$ values greater than 0.95 and smaller than 1.05. The results obtained with the use of model *or*3+*pr*3 show a slight increase of $\bar{x}$ values when compared with models *or*1+*pr*1 or *or*2+*pr*2. This seems to show that the stiffening effect has small influence. However, models *or*3 and *pr*3 should be considered theoretically more satisfactory, since they are nonlinear models. From the variation coefficient (cv) in Table 6, it can be observed that for the concrete models *c*11, *c*12, *c*13, *c*18 and *c*19, the cv values are smaller, generally below≈10%. The dispersion is not negligible but still acceptable. The results of Table 6 also seem to indicate that the hardening of ordinary and prestress reinforcement after the linear-elastic limit point does not have an important influence, since the results for *or*1+*pr*1 and *or*2+*pr*2 are very similar.

The previous analysis confirms that the use of the VATM, with appropriate σ-ε relationships for the materials, is appropriate for the prediction of the torsional strength of PC beams. This conclusion is logical since the beam is extensively cracked for high levels of loading (in this stage prestress reinforcement behaves like passive reinforcement).

The analysis of the results of Table 6, with respect to $\theta_{n,exp}/\theta_{n,th}$ ratios, shows a large range of values when compared with those for $T_{n,exp}/T_{n,th}$ ratios, as well as high values for cv (much over 10%). The dispersion of the results are larger than those observed for the $T_{n,exp}/T_{n,th}$ ratio. Generally, Table 6 shows that all the theoretical models appear to have some difficulty to predict adequately the deformation of the model beams for high loading levels. This was somehow expected because VATM assumes a fully cracked state of the beam from the beginning of loading. Among the concrete models, the results show that, for model *c*13+*or*3+*pr*3, the average value is optimal ($\bar{x}$=1.00), despite the high dispersion of the results (cv= 21.6%).

Table 6 $T_{n,exp}/T_{n,th}$ and $\theta_{n,exp}/\theta_{n,th}$ ratios

ci	*ri*	$T_{n,exp}/T_{n,th}$			$\theta_{n,exp}/\theta_{n,th}$		
		*or*1+*pr*1	*or*2+*pr*2	*or*3+*pr*3	*or*1+*pr*1	*or*2+*pr*2	*or*3+*pr*3
	$\bar{x}$	0.754	0.762	0.749	0.449	0.451	0.442
*c*01	s	0.103	0.109	0.082	0.169	0.168	0.155
	cv	13.72%	14.29%	10.97%	37.66%	37.13%	35.12%
	$\bar{x}$	0.844	0.847	0.864	0.668	0.685	0.623
*c*02	s	0.110	0.112	0.105	0.145	0.147	0.140
	cv	13.05%	13.18%	12.12%	21.74%	21.52%	22.49%
	$\bar{x}$	0.939	0.941	0.968	0.854	0.861	0.817
*c*03	s	0.102	0.103	0.108	0.200	0.214	0.173
	cv	10.89%	10.96%	11.14%	23.36%	24.80%	21.17%
	$\bar{x}$	0.883	0.886	0.901	0.712	0.726	0.671
*c*04	s	0.096	0.097	0.094	0.137	0.145	0.152
	cv	10.88%	10.98%	10.49%	19.27%	19.97%	22.70%
	$\bar{x}$	0.918	0.920	0.944	0.846	0.851	0.806
*c*05	s	0.095	0.096	0.100	0.171	0.177	0.168
	cv	10.34%	10.39%	10.55%	20.21%	20.85%	20.85%
	$\bar{x}$	0.930	0.931	0.957	0.862	0.857	0.824
*c*06	s	0.095	0.096	0.100	0.176	0.172	0.168
	cv	10.20%	10.26%	10.44%	20.38%	20.12%	20.43%
	$\bar{x}$	0.824	0.827	0.837	0.617	0.628	0.590
*c*07	s	0.102	0.104	0.091	0.149	0.148	0.160
	cv	12.35%	12.55%	10.91%	24.09%	23.64%	27.11%
	$\bar{x}$	0.865	0.867	0.884	0.742	0.747	0.702
*c*08	s	0.099	0.100	0.098	0.154	0.156	0.157
	cv	11.41%	11.51%	11.05%	20.75%	20.88%	22.29%
	$\bar{x}$	0.870	0.872	0.889	0.697	0.713	0.656
*c*09	s	0.101	0.102	0.097	0.149	0.152	0.155
	cv	11.64%	11.74%	10.96%	21.40%	21.37%	23.61%
	$\bar{x}$	0.883	0.886	0.902	0.667	0.670	0.651
*c*10	s	0.100	0.101	0.095	0.144	0.144	0.139
	cv	11.29%	11.43%	10.58%	21.61%	21.41%	21.39%
	$\bar{x}$	0.981	0.982	1.004	0.895	0.898	0.868
*c*11	s	0.098	0.098	0.097	0.198	0.202	0.183
	cv	9.97%	9.98%	9.61%	22.07%	22.45%	21.07%
	$\bar{x}$	0.959	0.960	0.983	0.951	0.956	0.915
*c*12	s	0.095	0.096	0.095	0.226	0.229	0.199
	cv	9.94%	9.96%	9.68%	23.79%	23.95%	21.74%
	$\bar{x}$	1.019	1.020	1.042	1.054	1.056	1.001
*c*13	s	0.104	0.104	0.101	0.274	0.272	0.216
	cv	10.23%	10.25%	9.70%	25.98%	25.77%	21.60%
	$\bar{x}$	1.072	1.072	1.095	1.137	1.142	1.073
*c*14	s	0.109	0.109	0.106	0.248	0.256	0.199
	cv	10.19%	10.19%	9.73%	21.81%	22.42%	18.56%
	$\bar{x}$	1.049	1.050	1.071	0.981	0.992	0.908
*c*15	s	0.105	0.105	0.104	0.234	0.253	0.163
	cv	10.01%	10.02%	9.72%	23.86%	25.54%	17.98%
	$\bar{x}$	0.855	0.859	0.867	0.633	0.637	0.614
*c*16	s	0.095	0.097	0.086	0.167	0.167	0.170
	cv	11.12%	11.28%	9.94%	26.36%	26.22%	27.73%
	$\bar{x}$	0.855	0.859	0.867	0.633	0.637	0.614
*c*17	s	0.095	0.097	0.086	0.167	0.167	0.170
	cv	11.12%	11.28%	9.94%	26.36%	26.22%	27.73%
	$\bar{x}$	1.011	1.012	1.030	0.814	0.817	0.787
*c*18	s	0.104	0.104	0.100	0.163	0.166	0.176
	cv	10.12%	10.30%	9.67%	20.05%	20.33%	22.33%
	$\bar{x}$	1.011	1.012	1.030	0.814	0.817	0.787
*c*19	s	0.104	0.104	0.100	0.163	0.166	0.176
	cv	10.32%	10.30%	9.67%	20.05%	20.33%	22.33%
	$\bar{x}$	0.903	0.906	0.913	0.689	0.690	0.672
*c*20	s	0.094	0.095	0.089	0.212	0.211	0.207
	cv	10.40%	10.45%	9.77%	30.80%	30.63%	30.78%

Table 7 Results from comparative analyses for model *c*13+*or*3+*pr*3

Beam	$T_{n,exp}$ kNm/m	$T_{n,th}$ kNm/m	$T_{n,exp}/T_{n,th}$	$\theta_{n,exp}$ °/m	$\theta_{n,th}$ °/m	$\theta_{n,exp}/\theta_{n,th}$
P3	55.8	60.8	0.92	3.14	2.67	1.18
P8	61.8	59.8	1.03	1.89	1.68	1.12
PA1R	21.9	20.0	1.09	2.97	4.63	0.64
PA2	28.7	29.9	0.96	2.88	3.41	0.85
PA3	34.2	34.8	0.98	2.68	2.84	0.94
PA4	37.0	39.2	0.94	2.94	2.53	1.16
PB1	21.9	19.2	1.14	4.50	5.02	0.90
PB2	27.4	28.2	0.97	2.77	3.61	0.77
PB3	32.7	32.4	1.01	3.09	3.19	0.97
PB4	37.7	37.2	1.01	2.66	2.94	0.91
PC1	19.7	16.8	1.18	5.22	5.23	1.00
PC2	28.7	25.2	1.14	3.37	3.97	0.85
PC3	32.9	28.5	1.16	4.71	3.46	1.36
PC4	38.7	32.1	1.21	3.83	3.12	1.23
P2	87.1	79.3	1.10	2.80	1.98	1.42
D1	396.0	466.4	0.85	1.73	2.35	0.74
D2	447.7	436.2	1.03	1.93	1.92	1.00
		$\bar{x}$ =	1.042		$\bar{x}$ =	1.001
		s =	0.101		*s* =	0.216
		cv =	9.70%		*cv* =	21.60%

Table 7 presents the results for $T_{n,exp}/T_{n,th}$ and $\theta_{n,exp}/\theta_{n,th}$ ratios obtained for model *c*13+*or*3+*pr*3. Fig. 4 presents bar graphs which allow a visual analysis of the dispersion of the results (from Table 7) comparatively to the optimal unit value. Table 7 and Fig. 4 confirm the good results observed in Table 6 for $T_{n,exp}/T_{n,th}$ ratio and the acceptable results for $\theta_{n,exp}/\theta_{n,th}$ ratio, by using model *c*13+*or*3+pr3.

In conclusion, among the best models for the torsional strength (*c*11, *c*12, *c*13, *c*18 and *c*19 with *or*3+*pr*3), it can be stated that model *c*13+*or*3+*pr*3 gives simultaneously the best results for the resistance torque and the corresponding twist. This model will be used for the next objectives of this study.

Fig. 5 presents both the experimental and all the theoretical T-θ curves for some test beams. Theoretical curve for model *c*13+*or*3+*pr*3 is highlighted. Fig. 4 clearly shows the high dispersion among the theoretical T-θ curves, mainly for high levels of loading. This high dispersion was also observed by Bernardo *et al.* (2012) for RC beams. Fig. 5 also shows that several models lead to torsional strength values that are not safe.

7. Comparative analysis with codes provisions

This section presents a comparative analysis with the predictions for the resistance torque computed through some codes of practice. The following codes of practice were considered: ACI 318R-05 (2005), European Codes MC 90 (1990) and EC 2 (2010). The objective is to analyze the degree of optimization of the theoretical model predictions in comparison with normative predictions that are expected to be more conservative. To compute the codes

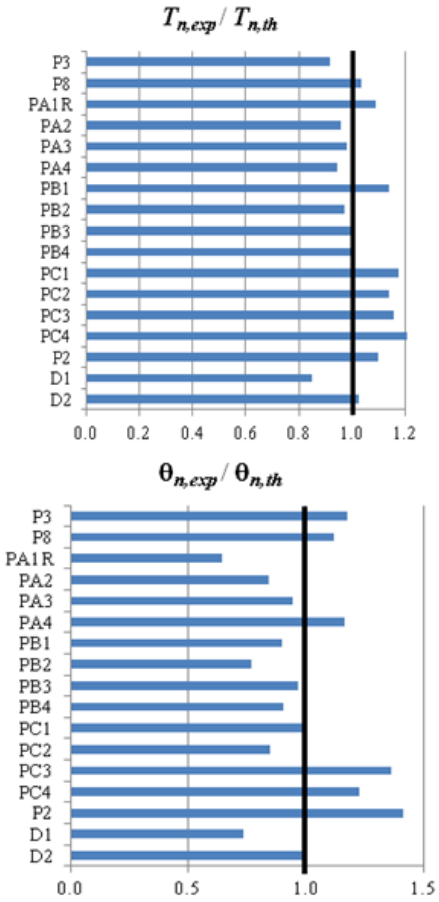

Fig. 4 Bar graphs with the results from Table 7

predictions, no safety factors were used and the strengths of the materials (steel and concrete) were characterized with their corresponding average values.

If a code of practice predicts brittle failure due to crushing of the concrete struts for a beam under torsion, then the corresponding torsional strength is computed by adopting the maximum values from the code for the compression stress in the concrete struts.

For this section, in addition to the reference beams analyzed in the previous section, other reference beams found in the literature are also added. As previously referred in Section 5, those beams just allow the study of their resistance torque (torsional strength), which is the purpose of this section. Then, twelve slender HSC beams with plain section and uniform longitudinal prestress tested by Wafa *et al.* (1995) were added in this section. The relevant characteristics of such beams to calculate the normative torsional strength are summarized in Table 8.

Table 9 summarizes the equations of the codes of practice used to compute the torsional strength of the PC test beams. For beams with longitudinal prestress, the longitudinal force in the ordinary reinforcement ($A_l f_{ly}$) is replaced by the total longitudinal force including the portion absorbed by the longitudinal prestress reinforcement: $A_l f_{ly}+A_p(f_{p0.1\%}-f_p)$ for ACI 318R-05 (2005) and $A_{si}f_{yd}+A_{pi}f_{pyd,net}$ for MC90 (1990) and EC2 (2010). The meaning of the parameters can be found in the codes. Table 9 also presents the normative ($T_{n,calc}$), the experimental

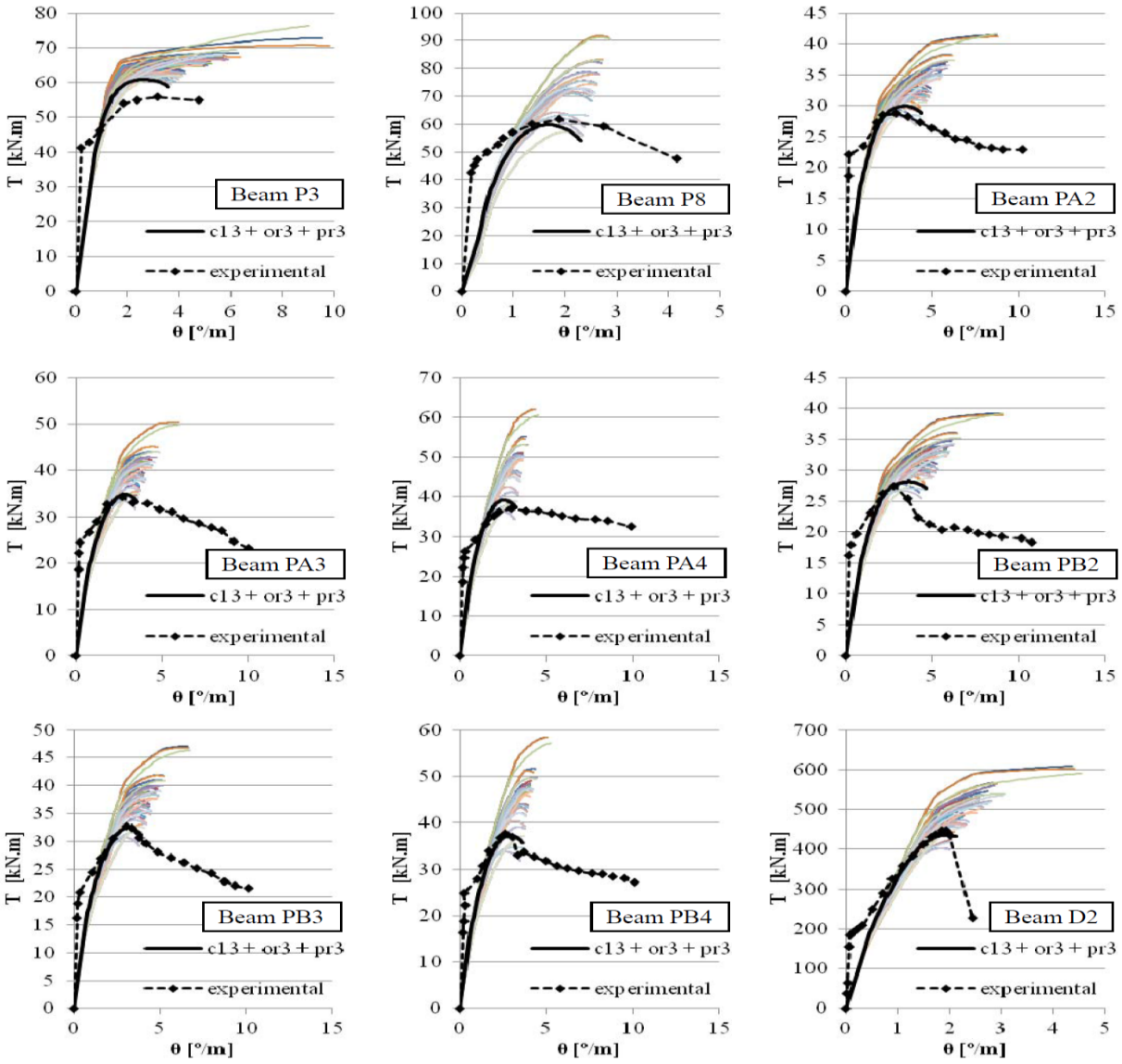

Fig. 5 Examples of T-θ curves

Table 8 Properties of the new test beams (Wafa *et al.* 1995)

Beam	Section type	x (cm)	y (cm)	x_1 (cm)	y_1 (cm)	A_{sl} (cm^2)	A_{st} / s (cm^2/m)	A_p (cm^2)	f_{cm} (MPa)	f_{lym} (MPa)	f_{tym} (MPa)	$f_{p0,1\%}$ (MPa)	f_{cp} (MPa)
H3AR	Plain	14.0	42.0	9.8	37.8	8.04	10.28	3.97	92.2	487	390	1816	8.3
H2A	Plain	17.0	34.0	12.8	29.8	8.04	12.57	3.97	91.9	487	390	1816	8.7
H1AR	Plain	24.0	24.0	19.8	19.8	8.04	12.57	3.97	94.7	487	390	1816	6.4
H3B	Plain	14.0	42.0	10.0	38.0	6.16	5.61	2.06	91.5	374	387	1841	4.0
H2B	Plain	24.0	24.0	13.0	30.0	6.16	6.04	2.06	95.6	374	387	1841	4.3
H1B	Plain	24.0	24.0	20.0	20.0	6.16	6.54	2.06	89.8	374	387	1841	4.3
M3A	Plain	14.0	42.0	9.8	37.8	8.04	10.28	3.97	69.9	487	390	1816	6.5
M2A	Plain	17.0	34.0	12.8	29.8	8.04	11.31	3.97	70.1	487	390	1816	6.2
M1A	Plain	24.0	24.0	19.8	19.8	8.04	12.57	3.97	72.5	487	390	1816	6.4
M3B	Plain	14.0	42.0	10.0	38.0	6.16	5.61	2.06	69.3	374	387	1841	3.2
M2B	Plain	17.0	34.0	13.0	30.0	6.16	6.04	2.06	69.7	374	387	1841	3.3
M1B	Plain	24.0	24.0	20.0	20.0	6.16	6.54	2.06	72.0	374	387	1841	3.2

($T_{n,exp}$) and the theoretical ($T_{n,th}$) torsional strength. This latter was computed in the previous section with model *c*13+*or*3+*pr*3 (Table 7).

Table 9 shows that ACI 318R-05 (2005) generally underestimates the torsional strength of PC beams, mainly for beams with high reinforcement ratios. It should be noted

Table 9 Torsional strength of test beams

model *c*13+*or*3+*pr*3			ACI 318R-05		MC 90		EC 2		
Beam	$T_{n,exp}$ (kNm)	$T_{n,th}$ (kNm)	$\frac{T_{n,exp}}{T_{n,th}}$	$T_{n,calc}$ (kNm)	$\frac{T_{n,exp}}{T_{n,calc}}$	$T_{n,calc}$ (kNm)	$\frac{T_{n,exp}}{T_{n,calc}}$	$T_{n,calc}$ (kNm)	$\frac{T_{n,exp}}{T_{n,calc}}$
P3	55.8	61.3	0.91	33.0(1)	1.69	31.9(1)	1.75	31.2(1)	1.79
P8	61.8	61.5	1.01	30.9	2.00	50.9(1)	1.22	55.9(1)	1.11
PA1R	21.8	20.0	1.09	14.0(1)	1.55	12.5(1)	1.74	12.7(1)	1.71
PA2	29.3	29.9	0.98	19.2	1.53	23.8(1)	1.23	24.2(1)	1.21
PA3	34.0	34.8	0.98	19.2	1.77	31.3(1)	1.09	31.8(1)	1.07
PA4	37.4	39.2	0.96	19.2	1.95	46.1(1)	0.81	34.3	1.09
PB1	22.2	19.2	1.16	13.1(1)	1.70	11.6(1)	1.90	11.5(1)	1.92
PB2	27.5	28.2	0.98	16.5	1.67	22.1(1)	1.25	22.0(1)	1.25
PB3	32.6	32.4	1.01	16.9	1.93	27.9(1)	1.17	27.7(1)	1.18
PB4	37.6	37.2	1.01	17.3	2.17	39.4(1)	0.96	39.3(1)	0.96
PC1	19.7	16.8	1.18	11.3(1)	1.74	10.1(1)	1.96	9.8(1)	2.01
PC2	28.6	25.2	1.14	13.9	2.05	18.7(1)	1.53	18.3(1)	1.56
PC3	32.8	28.5	1.15	14.1	2.32	23.2(1)	1.41	22.6(1)	1.45
PC4	38.5	32.1	1.20	14.3	2.70	32.9(1)	1.17	32.3(1)	1.19
H3AR	33.5	33.3	1.01	15.6	2.14	24.0(1)	1.39	23.9(1)	1.40
H2A	35.8	38.2	0.94	18.5	1.94	29.8(1)	1.20	30.7(1)	1.17
H1AR	38.4	38.1	1.01	21.3	1.80	37.0(1)	1.04	38.6	0.99
H3B	26.4	23.7	1.12	16.3	1.63	15.2(1)	1.74	15.0(1)	1.76
H2B	29.5	25.8	1.14	21.4(1)	1.79	23.8(1)	1.24	22.7(1)	1.30
H1B	31.3	27.4	1.14	21.4	1.46	20.2(1)	1.55	20.2(1)	1.56
M3A	30.0	29.8	1.01	13.6	2.20	26.4(1)	1.13	26.3(1)	1.14
M2A	31.9	32.1	1.00	16.2	1.98	30.5(1)	1.05	33.1(1)	0.97
M1A	35.4	35.6	1.00	18.7	1.90	37.0(1)	0.96	38.6(1)	0.92
M3B	24.5	21.9	1.12	14.2	1.73	16.2(1)	1.51	16.1(1)	1.53
M2B	26.2	23.4	1.12	16.7	1.57	17.9(1)	1.46	19.1(1)	1.37
M1B	28.9	25.3	1.14	19.2	1.51	21.3(1)	1.36	22.1(1)	1.31
P2	87.1	78.2	1.12	59.2(1)	1.47	50.2(1)	1.74	51.0(1)	1.71
D1	396.0	419.1	0.95	404.8	0.98	371.6(1)	1.07	438.0(1)	0.90
D2	447.7	401.5	1.12	370.1	1.21	360.6(1)	1.24	421.7(1)	1.06
(1)Ductile failure		$\bar{x}$ =	1.056	$\bar{x}$ =	1.782	$\bar{x}$ =	1.340	$\bar{x}$ =	1.330
		s =	0.085	*s* =	0.352	*s* =	0.302	*s* =	0.081
		cv =	8.03%	*cv* =	19.75%	*cv* =	22.50%	*cv* =	23.63%

ACI 318R-05 (2005),

$$A_t = \frac{A_t}{s} p_h \frac{f_{yv}}{f_{yl}} \cot g^2\theta \rightarrow \theta$$

$$T_n = \frac{2A_o A_t f_{yv}}{s} \cot g\,\theta$$

Brittle failure:

$$T_n = \frac{8\sqrt{f_c'}1{,}7A_{oh}^{\ 2}}{p_h}$$

MC 90 (1990),

$$tg\,\theta_i = \sqrt{\frac{A_{swi} f_{ywd} z_i / s}{A_{si} f_{yd}}} \rightarrow \theta$$

$$T_n = T_{Rtwi} = 2F_{Rtwi} A_{ef} / z_i$$

$$F_{Rtwi} = A_{Swi} f_{yd} \cot g\,\theta_i \frac{z_i}{s}$$

Brittle failure:

$$T_{Rcwi} = 2F_{Rcwi} \sin\theta_i A_{ef} / z_i$$

$$F_{Rcwi} = f_{cd2} t_i z_i \cos\theta_i$$

EC2 (2010),

$$tg\,\theta = \sqrt{\frac{A_{st,i} f_{ywd} u_k}{s\sum A_{sl} f_{yd}}} \rightarrow \theta$$

$$T_n = T_{Rd2} = 2A_k \left(f_{ywd} A_{sw} / s\right) \cot g\,\theta$$

Brittle failure:

$$T_{Rd1} = 2\nu f_{cd} t A_k \sin\theta\cos\theta$$

that, according to Bernardo and Lopes (2009, 2013), the range of torsional reinforcement ratio compatible with some torsional ductility is very narrow. This shows that brittle failure is a common situation in the current cases of beams under high torsional moments. For such beams, ACI 318R-05 (2005) seems to be very conservative. Except for Beams D1 and D2 (large hollow beams), ACI 318R-05 (2005) generally provides safe values for the torsional strength ($\bar{x}$=1.78 for $T_{n,exp}$ /$T_{n,calc}$ ratio) and with high deviations (*cv*=19.8%).

Table 9 shows that MC 90 (1990) and EC 2 (2010) generally also underestimate the torsional strength of PC beams ($\bar{x}$=1.33 to 1.34), although not as much as ACI code. However, all the test beams would lead to a ductile failure according to MC 90 (1990) and EC 2 (2010) (failure due to the yielding of the reinforcement). The experimental results of the test beams show that the majority of them had a brittle failure. Table 9 also shows that the deviation of $T_{n,exp}$ /$T_{n,calc}$ ratio is large (*cv*≈23 to 24%).

Table 9 also shows that model *c*13+*or*3+*pr*3 provides much more accurate values for the torsional strength and with a coefficient of variation lesser than 10%.

Fig. 6 presents graphs of the ratios $T_{n,exp}$ /$T_{n,calc}$ and $T_{n,exp}$ /$T_{n,th}$ ($T_{n,th}$ computed with model *c*13+*or*3+*pr*3) as a function of the compressive strength of concrete (f_{cm}) for each code. Generally, Fig. 6 confirms graphically the same conclusions previously stated based on the analysis of Table 9. All the codes are conservative for the majority of the test beams, especially for beams with high torsional reinforcement ratio. However, ACI 318R-05 (2005) is more conservative than MC 90 (1990) and EC 2 (2010).

Fig. 6 shows that the deviations of the results are high between the test beams studied. Fig. 6 also confirms that VATM with model *c*13+*or*3+*pr*3 provides closer predictions for torsional design when compared to those of the studied codes.

8. Conclusions

In the first part of this article, a general computing procedure based on the VATM to compute the ultimate behavior of PC beams under torsion is presented. In order to extend the application of the VATM, the original equations were rewritten to cover both longitudinal and/or transversal PC beams under torsion. Despite no experimental data for

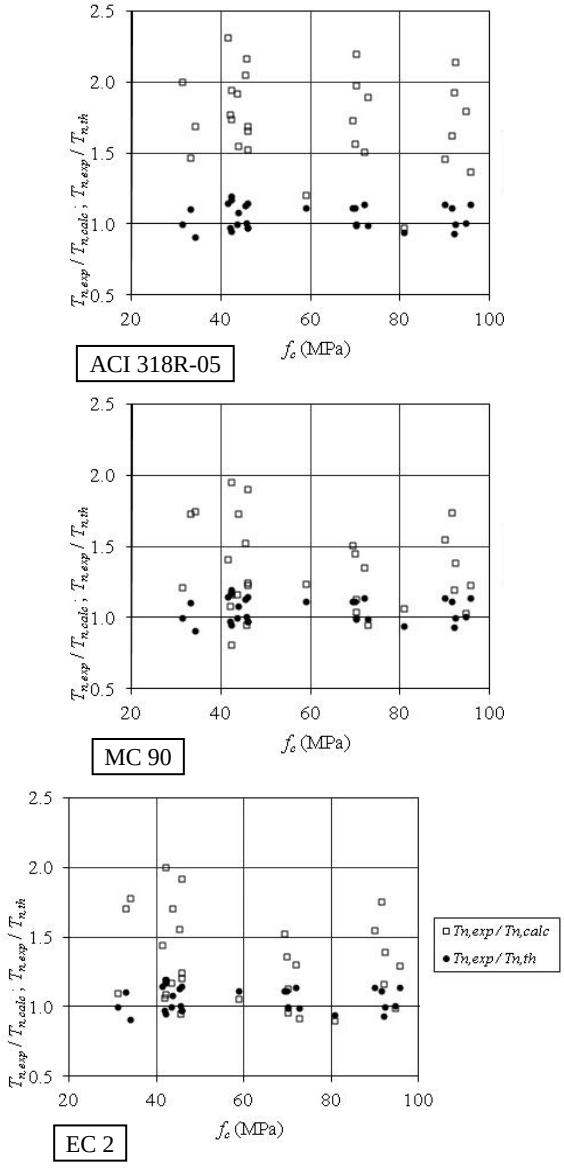

Fig. 6 $T_{n,exp}$ /$T_{n,calc}$ and $T_{n,exp}$/$T_{n,th}$ ratios

transversally PC beams were found for this study, such extension of the VATM can be useful for future researches involving RC beams under torsion with transversal prestress.

In the second part of this article, several σ-ε relationships for the materials (concrete and reinforcements) were checked with the help of numerical simulations in order to compute the ultimate behavior of tested PC beams (with longitudinal prestress) under torsion. The theoretical procedure was based on the VATM formulation. Based on the obtained results and from comparative analysis, the authors found that some theoretical models lead to good predictions for the torsional strength of PC beams under torsion. In particular, model *c*13+*or*3+*pr*3 provides simultaneously acceptable predictions for the twist corresponding to the torsional strength.

Model *c*13 for concrete struts incorporates the softened σ-ε relationship proposed by Belarbi and Hsu (1991) and the reduction factors proposed by Hsu (1993) (see Tables 1 and 2). Model *or*3+*pr*3 incorporates the stiffened σ-ε relationships from Belarbi and Hsu (1994) for the ordinary reinforcement and from Ramberg-Osgood, proposed by Hsu and Mo (1985), for the prestress reinforcement (see Table 4).

As referred in Section 2, in a previous study Bernardo *et al.* (2012) tested several σ-ε relationships for concrete in compression and ordinary reinforcement in tension to study the behaviour of RC beams under torsion. Their analysis was performed with a much great number of test beams than the one used in the present study with PC beams. In the referred study, the authors found that the model which provides the best predictions for the maximum torque and corresponding twist is the one that incorporates the σ-ε relationships for compressed concrete in struts proposed by Belarbi and Hsu (1991) with softening coefficients proposed by Zang and Hsu (1998) and the σ-ε relationship for ordinary reinforcement in tension proposed by Belarbi and Hsu (1994). In the present study, the previous model corresponds to model *c*14+*or*3 (see Table 3, without prestress reinforcement). When compared with model *c*13+*or*3+*pr*3, found in the present study to be the best model, the unique difference is related with the softening coefficient. However, in the present study, model *c*14+*or*3+*pr*3 is not one of the best models for PC beams (Section 6). Despite the limited number of PC test beams used in this study, the combined results from this study and from the previously referred study for RC beams seems to show that the expected differences between RC and PC beams under torsion, as referred in Section 2, exist and are reflected in the σ-ε relationships of the materials incorporated in the VATM.

In the last part of this article, the predictions for the torsional strength of the test beams, computed with model *c*13+*or*3+*pr*3, were compared with those computed from some codes of practice (ACI 318R-05 2005, MC 90 1990,d EC 2 2010).

The results show that ACI 318R-05 (2005) generally underestimates the torsional resistance of PC beams, mainly for beams with high reinforcement ratio. For such beams, ACI 318R-05 (2005) provides values highly below the experimental strengths and with large deviations. Both MC 90 (1990) and EC 2 (2010) generally also underestimate the torsional strength of PC beams, although not as much as ACI 318R-05 (2005). Nevertheless, the dispersion of the results is also high.

When compared with the predictions from codes, the theoretical model *c*13+*or*3+*pr*3 provides good values for the torsional strength, which would lead to better optimized designs.

In this study it was not possible to compare the predictions from the computing procedure for transversally PC beams since no experimental results were found in the literature. Therefore, experimental tests of this type of beams are need.

References

ACI Committee 318 (2005), Building Code Requirements for

Reinforced Concrete, (ACI 318-05) and Commentary (ACI 318R-05), American Concrete Institute, Detroit, MI.

AlNuaimi, A.S., Al-Jabri, K.S. and Hago, A. (2008), "Comparison between solid and hollow reinforced concrete beams", *Mater. Struct.*, **41**(2), 269-286.

Andrade, A.M., Bernardo, L.F.A. and Lopes, S.M.R. (2011**),** "TORQUE_MTEAV: computing tool to evaluate the ultimate behaviour of reinforced and prestressed concrete beams in torsion", *Proceedings of the International Conference on Recent Advances in Nonlinear Models-Structural Concrete Aplications (CoRAN 2011)*, November, Coimbra, Portugal.

Bairan Garcia, J.M. and Mari Bernat, A.R. (2006a), "Coupled model for the non-linear analysis of anisotropic sections subjected to general 3D loading. Part 1: Theoretical formulation", *Comput. Struct.*, **84**(31-32), 2254-2263.

Bairan Garcia, J.M. and Mari Bernat, A.R. (2006b), "Coupled model for the nonlinear analysis of sections made of anisotropic materials, subjected to general 3D loading. Part 2: Implementation and validation", *Comput. Struct.*, **84**(31-32), 2264-2276.

Belarbi, A. and Hsu T.C. (1994), "Constitutive laws of concrete in tension and reinforcing bars stiffened by concrete", *Struct. J. Am. Concrete Inst.*, **91**(4), 465-474.

Belarbi, A. and Hsu, T.C. (1991), "Constitutive laws of softened concrete in biaxial tension-compression", Research Report UHCEE 91-2, Univ. of Houston, Houston, Texas.

Belarbi, A. and Hsu, T.C. (1995), "Constitutive laws of softened concrete in biaxial tension-compression", *Struct. J. Am. Concrete Inst.*, **92**(5), 562-573.

Bernardo, L.F.A. and Lopes S.M.R. (2004), "Neutral axis depth versus flexural ductility in high-strength concrete beams", *ASCE J. Struct. Eng.*, **130**(3), 452-459.

Bernardo, L.F.A. and Lopes, S.M.R. (2008), "Behaviour of concrete beams under torsion-NSC plain and hollow beams", *Mater. Struct.*, **41**(6), 1143-1167.

Bernardo, L.F.A. and Lopes, S.M.R. (2009), "Torsion in HSC hollow beams: strength and ductility analysis", *ACI Struct. J.*, **106**(1), 39-48.

Bernardo, L.F.A. and Lopes, S.M.R. (2011a), "Theoretical behaviour of HSC sections under torsion", *Eng. Struct.*, **33**(12), 3702-3714.

Bernardo, L.F.A. and Lopes, S.M.R. (2011b), "High-strength concrete hollow beams strengthened with external transversal steel reinforcement under torsion", *J. Civil Eng. Manage.*, **17**(3), 330-339.

Bernardo, L.F.A. and Lopes, S.M.R. (2013), "Plastic analysis and twist capacity of high-strength concrete hollow beams under pure torsion", *Eng. Struct.*, **49**, 190-201.

Bernardo, L.F.A., Andrade, J.M.A. and Lopes, S.M.R. (2012a)**,** "Softened truss model for reinforced NSC and HSC beams under torsion: a comparative study", *Eng. Struct.*, **42**(12), 278-296.

Bernardo, L.F.A., Andrade, J.M.A. and Lopes, S.M.R. (2012b), "Modified variable angle truss-model for torsion in reinforced concrete beams", *Mater. Struct.*, **45**(12), 1877-1902.

Bernardo, L.F.A., Taborda, C.S.B. and Andrade, J.M.A. (2015a) "Ultimate torsional behaviour of axially restrained RC beams", *Comput. Concrete*, **16**(1), 67-97.

Bernardo, L.F.B., Taborda, C.S.B. and Gama, J.M.R. (2015b) "Parametric analysis and torsion design charts for axially restrained RC beams", *Struct. Eng. Mech.*, **55**(1), 1-27.

Collins, M.P. and Poraz, A. (1989), "Shear design for high strength concrete", Bulletin d'Information N.º 193-Design Aspects of High Strength Concrete, CEB, 75-83.

Comité Euro-International du Béton (CEB) (1990), CEB-FIP MODEL CODE 1990.

Hognestad, E. (1952), "What do we know about diagonal tension and web reinforcement in concrete?", Circular Series, 64, University of Illinois, Engineering Exp. Station, III.

Hsu, T.T.C. (1984), *Torsion of Reinforced Concrete*, Van Nostrand Reinhold Company.

Hsu, T.T.C. (1993), *Unified Theory of Reinforced Concrete*, CRC Press, Inc., Boca Raton.

Hsu, T.T.C. and Mo, Y.L. (1985), "Softening of concrete in torsional members-prestressed concrete", *ACI J. Pr.*, **82**(5), 603-615.

Jeng, C.H. and Hsu, T.T.C. (2009), "A softened membrane model for torsion in reinforced concrete members", *Eng. Struct.*, **31**(9), 1944-54.

Jeng, C.H., Chiu, H.J. and Chen, C.S. (2010), "Modeling the initial stresses in prestressed concrete members under torsion", *2010 Structures Congress*, ASCE, 1773-1781.

Jeng, C.H., Chiu, H.J. and Peng, S.F. (2013), "Design formulas for cracking torque and twist in hollow reinforced concrete members", *ACI Struct. J.*, **110**(3), 457-468.

Jeng, C.H., Peng, X. and Wong, Y.L. (2011), "Strain gradient effect in RC elements subjected to torsion", *Mag. Concrete Res.*, **63**(5), 343-356.

Lopes, S.M.R. and Bernardo, L.F.A. (2009), "Twist behavior of high-strength concrete hollow beams-formation of plastic hinges along the length", *Eng. Struct.*, **31**(1), 138-149.

Lopes, S.M.R., Bernardo, L.F.A. and Costa, R.J.T. (2015a), "Reinforced concrete membranes under shear: global behaviour", *Exp. Techniq.*, **39**, 30-43.

Lopes, S.M.R., Bernardo, L.F.A. and Costa, R.J.T. (2015b), "Reinforced concrete membranes under shear: ultimate behaviour and influence of thickness", *Exp. Techniq.*, **39**, 44-56.

McMullen, A.E. and El-Degwy, W.M. (1985), "Prestressed concrete tests compared with torsion theories", *PCI J.*, **30**(5), 96-127.

Mikame, A., Uchida, K. and Noguchi, H. (1991), "A study of compressive deterioration of cracked concrete", *Proceedings of the International Workshop on Finite Element Analysis of Reinforced Concrete*, Columbia University, New York, N.Y.

Mitchell, D. and Collins, M.P. (1974), "The behavior of structural concrete beams in pure torsion", Civil Engineering Publication No.74-06, Department of civil Engineering, University of Toronto, March.

Miyahara, T., Kawakami, T. and Maekawa, K. (1988), "Nonlinear behavior of cracked reinforced concrete plate element under uniaxial compression", *Concrete Lib. Int. JPN Soc. Civil Eng.*, **11**, 306-319.

Mostofinejad, D. and Behzad, T.S. (2011), "Nonlinear modeling of RC beams subjected to torsion using smeared crack model", *The Twelfth East Asia-Pasific Conference on Structural Engineering and Construction (EASEC-12)*, Hong Kong SAR, China, January.

Navarro Gregori, J., Sosa, P.M., Prada, M.A.F. and Filippou, F.C. (2007), "A 3D numerical model for reinforced and prestressed concrete elements subjected to combined axial, bending, shear and torsion loading", *Eng. Struct.*, **29**(12), 3404-3419.

NP EN 1992-1-1 (2010), Eurocode 2: Design of Concrete Structures - Part 1: General Rules and Rules for Buildings.

Rahal, K.N. and Collins, M.P. (1996), "Simple model for predicting torsional strength of reinforced and prestressed concrete sections", *ACI Struct. J.*, **93**(6), 658-666.

Ueda, M., Noguchi, H., Shirai, N. and Morita, S. (1991), "Introduction to activity of new RC", *Proceedings of the International Workshop on Finite Element Analysis of Reinf. Concrete*, Columbia Univ., New York, N.Y.

Valipour, H.R. and Foster, S.J. (2010), "Nonlinear analysis of 3D reinforced concrete frames: effect of section torsion on the global response", *Struct. Eng. Mech.*, **36**(4), 421-445.

Vecchio, F.J. (2000a), "Disturbed stress field model for reinforced

concrete: formulation", *J. Struct. Eng.*, **126**(9), 1070-1077.
Vecchio, F.J. (2000b), "Analysis of shear-critical reinforced concrete beams", *Struct. J. Am. Concrete Inst.*, **97**(1), 102-110.
Vecchio, F.J. and Collins, M.P. (1982), "The response of reinforced concrete to in-plane shear and normal stresses", Publication N.º 82-03, Department of Civil Engineering, University of Toronto, Toronto, Canada.
Vecchio, F.J. and Collins, M.P. (1986), "The modified compression-field theory for reinforced concrete elements subjected to shear", *J. Am. Concrete Inst.*, **83**(2), 219-231.
Vecchio, F.J., Collins, M.P. and Aspiotis, J. (1994), "High-strength concrete elements subjected to shear", *Struct. J. Am. Concrete Inst.*, **91**(4), 423-433.
Wafa, F.F., Shihata, S.A., Ashour, S.A. and Akhtaruzzaman, A.A. (1995), "Prestressed high-strength concrete beams under torsion", *J. Struct. Eng.*, **121**(9), 1280-1286.
Zhang, L.X. and Hsu, T.T.C. (1998), "Behaviour and analysis of 100 MPa concrete membrane elements", *J. Struct. Eng.*, ASCE, **124**(1), 24-34.
Zhu, R.R.H., Hsu, T.T.C. and Lee, J.Y. (2001), "Rational shear modulus for smeared-crack analysis of reinforced concrete", *Struct. J. Am. Concrete Inst.*, **98**(4), 443-450.

PL

Nomenclature

A_c area limited by the external perimeter of the cross section
$A_{c,\text{hom}}$ area of homogenized concrete
A_h area of the hollow part of the cross section
A_l total area of the longitudinal ordinary reinforcement
A_o area limited by the center line of the flow of shear stresses
A_p, A_{pl} total area of the longitudinal prestress reinforcement
A_{pt} area of one leg of the transversal prestress reinforcement
A_{sl}, A_l total area of longitudinal ordinary reinforcement
A_{st} area of one leg of transversal ordinary reinforcement
A_t area of one leg of transversal ordinary and prestress reinforcement
ci combination i
cv coefficient of variation
E_c Young's modulus of concrete
E_p Young's modulus of prestress reinforcement
E_{pl} Young's modulus of longitudinal prestress reinforcement
E_{pt} Young's modulus of transversal prestress reinforcement
E_s Young's modulus of ordinary reinforcement
$F_{pi,t}$ initial transversal prestress force
f_c' cylinder compressive strength of concrete
f_c, f_{c2} principal compression stress of concrete
f_{cm} average concrete compressive strength
f_{cp} average stress in the concrete due to prestress
f_l tensile stress of longitudinal ordinary reinforcement
f_{lym} average yielding stress of longitudinal reinforcement
f_p tensile stress of prestress reinforcement
f_{pi} initial stress in the prestress reinforcement
$f_{pi,l}$ initial stress in the longitudinal prestress reinforcement
$f_{pi,t}$ initial stress in the transversal prestress reinforcement
$f_{p0.1\%}$ stress of prestress reinforcement corresponding to $\varepsilon_{p0.1\%}$
$f_{pl0.1\%}$ conventional stress of longitudinal prestress reinforcement
$f_{pt0.1\%}$ conventional stress of transversal prestress reinforcement
f_{pt} tensile strength of prestress reinforcement
f_s tensile stress of ordinary reinforcement
f_{sly}, f_{ly} yielding stress of longitudinal ordinary reinforcement
f_{sty} yielding stress of transversal ordinary reinforcement
f_{st} tensile strength of ordinary reinforcement
f_{sy} yielding stress of ordinary reinforcement
f_t tensile stress of transversal ordinary reinforcement
f_{tym} average yielding stress of transversal reinforcement
k_1 ratio between the medium stress and the maximum stress in the concrete strut
orj σ-ε relationship j for ordinary reinforcement
prj σ-ε relationship j for prestress reinforcement
p_o perimeter of area A_o
s standard deviation
s_p spacing of the transversal prestress reinforcement
s_t, s spacing of the transversal ordinary reinforcement
T torque; torsional moment
$T_{n,calc}$ normative value for the torsional strength
$T_{n,exp}$ experimental value for the torsional strength
$T_{n,th}$ theoretical value for the torsional strength
t thickness of the walls of the cross hollow section
t_d effective thickness of the walls (struts)
u_p perimeter of the transversal prestress reinforcement
u_t perimeter of the transversal ordinary reinforcement
x width of the cross section
$\bar{x}$ average value
x_1 distance between centerlines of vertical legs of the closed stirrup
x_2 distance between centerlines of horizontal legs of the closed stirrup
y height of the cross section
α angle of the concrete struts
β reduction factor
β_σ reduction factor for stress
β_ε reduction factor for strain
ε strain
ε_{c1} principal tension strain of concrete
ε_c, ε_{c2} principal compression strain of concrete
ε_{cu} ultimate compression strain of concrete
ε_d strain at the center line of the flow of shear stresses
$\varepsilon_{dec,l}$ strain in the longitudinal prestress reinforcement at decompression
$\varepsilon_{dec,t}$ strain in the transversal prestress reinforcement at decompression
ε_{ds} strain at the surface of the diagonal concrete strut
ε_l strain of the longitudinal ordinary reinforcement
ε_{li} initial strain in the longitudinal ordinary reinforcement due to prestress
ε_o strain corresponding to the peak stress f_c'

$\varepsilon_{p0.1\%}$ conventional strain (0.1%) of prestress reinforcement
ε_p tensile strain of prestress reinforcement
$\varepsilon_{pi,l}$ initial strain in the longitudinal prestress reinforcement due to prestress
$\varepsilon_{pi,t}$ initial strain in the transversal prestress reinforcement due to prestress
ε_{pl} strain in the longitudinal prestress reinforcement
ε_{pt} strain in the transversal prestress reinforcement
ε_{pu} ultimate strain of prestress reinforcement
ε_s tensile strain of ordinary reinforcement
ε_{su} ultimate strain of ordinary reinforcement
ε_t strain of the transversal ordinary reinforcement
ε_{ti} initial strain in the transversal ordinary reinforcement due to prestress
σ normal stress
σ_d stress in the diagonal concrete strut
σ_l stress in the longitudinal ordinary reinforcement
σ_{pl} stress in the longitudinal prestress reinforcement
σ_{pt} stress in the transversal prestress reinforcement
σ_t stress in the transversal ordinary reinforcement
ρ_l longitudinal ordinary reinforcement ratio
ρ_{pl} longitudinal prestress reinforcement ratio
ρ_{pt} transversal prestress reinforcement ratio
ρ_t transversal ordinary reinforcement ratio
θ angle of twist per unit length
$\theta_{n,exp}$ experimental value of twist corresponding to $T_{n,exp}$
$\theta_{n,th}$ theoretical value of twist corresponding to $T_{n,th}$